CANCER

Tumor-derived exosomes modulate PD-L1 expression in monocytes

Franziska Haderk,[1] Ralph Schulz,[1] Murat Iskar,[1] Laura Llaó Cid,[1] Thomas Worst,[2] Karolin V. Willmund,[1] Angela Schulz,[1,3] Uwe Warnken,[3] Jana Seiler,[4] Axel Benner,[5] Michelle Nessling,[6] Thorsten Zenz,[7] Maria Göbel,[8] Jan Dürig,[8] Sven Diederichs,[4,9,10] Jérôme Paggetti,[11] Etienne Moussay,[11] Stephan Stilgenbauer,[12] Marc Zapatka,[1] Peter Lichter,[1] Martina Seiffert[1]*

In chronic lymphocytic leukemia (CLL), monocytes and macrophages are skewed toward protumorigenic phenotypes, including the release of tumor-supportive cytokines and the expression of immunosuppressive molecules such as programmed cell death 1 ligand 1 (PD-L1). To understand the mechanism driving protumorigenic skewing in CLL, we evaluated the role of tumor cell–derived exosomes in the cross-talk with monocytes. We carried out RNA sequencing and proteome analyses of CLL-derived exosomes and identified noncoding Y RNA hY4 as a highly abundant RNA species that is enriched in exosomes from plasma of CLL patients compared with healthy donor samples. Transfer of CLL-derived exosomes or hY4 alone to monocytes resulted in key CLL-associated phenotypes, including the release of cytokines, such as C-C motif chemokine ligand 2 (CCL2), CCL4, and interleukin-6, and the expression of PD-L1. These responses were abolished in Toll-like receptor 7 (TLR7)–deficient monocytes, suggesting exosomal hY4 as a driver of TLR7 signaling. Pharmacologic inhibition of endosomal TLR signaling resulted in a substantially reduced activation of monocytes in vitro and attenuated CLL development in vivo. Our results indicate that exosome-mediated transfer of noncoding RNAs to monocytes contributes to cancer-related inflammation and concurrent immune escape via PD-L1 expression.

INTRODUCTION

Tumor-promoting inflammation and escape from immune-mediated tumor destruction have been recognized as hallmarks of cancer (*1*). Tumor-associated macrophages are key players in these processes and are currently being explored as therapeutic targets in a number of cancers (*2*).

Chronic lymphocytic leukemia (CLL) is a malignancy of mature $CD5^+CD19^+$ B lymphocytes that is associated with an inflammatory milieu and defective immune responses (*3*, *4*). Monocytes in the blood of CLL patients as well as macrophages in lymphoid organs are skewed toward immunosuppressive phenotypes, including the up-regulation of the immune regulatory molecules programmed cell death 1 ligand 1 (PD-L1) and indoleamine 2,3-dioxygenase 1 (IDO1) (*5*, *6*). Depletion of monocytes and macrophages, or treatment with anti–PD-L1 antibodies, attenuates tumor development in the *E*μ-TCL1 mouse model of CLL, highlighting the relevance of immune control in this disease (*7*, *8*). So far, the mechanisms of how CLL cells influence the development and activity of monocytes and macrophages are not understood.

Cancer cell–derived extracellular vesicles (EVs) are key players for communication with the tumor microenvironment and are reported to promote anti- and protumorigenic effects in immune cells and other nontumor bystander cells (*9*–*11*). In general, two types of EVs are distinguished, namely, 50- to 150-nm-sized exosomes of endosomal origin and 100- to 1000-nm-sized microvesicles directly budding from the plasma membrane (*9*, *12*). Both can promote local and systemic effects by interaction with target cells (*12*–*14*). This is especially relevant for RNA shuttled by cancer-derived EVs, given that RNA remains functional upon EV encapsulation and uptake by recipient cells (*15*–*17*). RNA analyses of exosomes have previously revealed an accumulation of small RNA species, including microRNAs (miRNAs), Y RNAs, ribosomal RNAs (rRNAs), and transfer RNAs (tRNAs) (*18*, *19*). Y RNAs are evolutionary conserved, RNA polymerase III–transcribed, noncoding RNAs (83 to 112 nucleotides (nt) in length) that are involved in DNA replication and RNA quality control (*20*, *21*). Fragmentation of Y RNAs to about 30-nt sequences was observed upon cellular stress and apoptosis (*22*, *23*). However, little is known about the role of EV-encapsulated Y RNAs and their effect on target cells in the microenvironment.

CLL cells have been shown to secrete EVs upon B cell receptor stimulation, and tumor-derived EVs have been detected in the blood of CLL patients (*24*, *25*). Uptake of CLL-derived EVs by stromal cells has been shown to promote activation of mechanistic target of rapamycin (mTOR)/AKT signaling (*25*) and the induction of an inflammatory phenotype that is associated with enhanced tumor growth in mice (*26*). We have previously demonstrated monocytes and macrophages to be the major targets of CLL-derived exosomes (*26*), but little is known about how exosomes influence the function of these immune cells.

Here, we isolated exosomes from blood plasma samples of CLL patients and from culture supernatant of a CLL cell line and characterized their content by proteome analysis and RNA sequencing. Focusing on

[1]Department of Molecular Genetics, German Cancer Research Center (DKFZ), Heidelberg, Germany. [2]Division of Signaling and Functional Genomics, DKFZ, Heidelberg, Germany. [3]Genomics and Proteomics Core Facility, DKFZ, Heidelberg, Germany. [4]Division of RNA Biology and Cancer (B150), DKFZ, Heidelberg, Germany. [5]Division of Biostatistics, DKFZ, Heidelberg, Germany. [6]Central Unit Electron Microscopy, DKFZ, Heidelberg, Germany. [7]Department of Molecular Therapy in Hematology and Oncology and Department of Translational Oncology, National Center for Tumor Diseases (NCT); DKFZ; and Department of Medicine V, University Hospital Heidelberg, Heidelberg, Germany. [8]Department of Hematology, Essen University Hospital, Essen, Germany. [9]Division of Cancer Research, Department of Thoracic Surgery, Medical Center–Faculty of Medicine, University of Freiburg, Freiburg, Germany. [10]German Cancer Consortium (DKTK), Freiburg, Germany. [11]Laboratory of Experimental Cancer Research, Luxembourg Institute of Health, Luxembourg City, Luxembourg. [12]Department of Internal Medicine III, University Hospital Ulm, Ulm, Germany.
*Corresponding author. Email: m.seiffert@dkfz.de

their functional relevance, we treated monocytes ex vivo with exosomes and monitored uptake as well as exosome-mediated responses by confocal microscopy, flow cytometry, and cytokine quantification. We have identified the Y RNA hY4 as a highly abundant RNA in CLL-derived exosomes and showed that both exosomes and exogenous hY4 induce PD-L1 expression and cytokine release in monocytes and thus contribute to a tumor-supportive microenvironment in CLL. Inhibition of Toll-like receptor (TLR) signaling in mice reduced CLL development and might therefore be of therapeutic interest.

RESULTS

B cell–derived exosomes are enriched in plasma of CLL patients

Exosomes from blood plasma of CLL patients (see table S1 for patient information) or healthy donors as well as from culture supernatant of the CLL cell line MEC-1 were isolated via serial centrifugation, as described previously (*27*). Confirming previously published results (*26*–*28*), negative stain electron microscopy showed vesicles in typical cup-shaped morphology. Their sizes ranged from 30 to 350 nm; they were positive for exosome markers RAB5a and HSP70, and immunoelectron microscopy demonstrated human leukocyte antigen–antigen D–related (HLA-DR) expression of exosomes (Fig. 1, A to D, and fig. S1A). Quantification of absolute particle numbers in blood plasma via nanoparticle tracking analysis (NTA) showed no significant difference in exosome counts for CLL patients compared with healthy donors ($P = 0.30$), with median concentrations of 1.0×10^{10} exosomes per milliliter of plasma for both groups (Fig. 1E). This was confirmed by quantification of CD81, a general exosome marker ($P = 0.65$; fig. S1B). Furthermore, absolute exosome counts determined by NTA did not correlate with age ($P = 0.48$) or leukocyte count ($P = 0.09$) of individuals, and no significant difference in CLL patients with good or bad prognosis ($P = 0.11$) was observed (fig. S1, C to E). However, for platelet counts, a significant correlation with absolute exosome numbers ($r = 0.54$, $P = 0.01$) was detected (fig. S1F), suggesting that most of the exosomes in our plasma preparations were platelet-derived.

Proteome profiling of plasma-derived exosomes from CLL patients and healthy donors was performed via mass spectrometry. In total, 347 proteins were identified by MaxQuant analysis in plasma exosomes of at least three of four samples in either group. Label-free quantification and comparison among groups revealed 91 proteins with a significant and at least twofold difference between CLL and healthy donor exosomes. Among them, various vesicle markers such as annexins, actin- and Ras-related proteins, and 14-3-3 signaling proteins were elevated in CLL-derived exosomes (table S2). This suggests an altered composition of plasma exosomes in CLL, despite unchanged overall exosome levels.

Exosomes derived from malignant B cells have been previously shown to present CD20 on their surface (*26*, *28*). CD20, as a B cell marker, is expressed on CLL cells and was enriched in two of four of the tested plasma exosome preparations of CLL patients. Therefore, we evaluated whether quantification of CD20 by enzyme-linked immunosorbent assay (ELISA) can be used as an indicator for the amount of B cell–derived exosomes in blood plasma. Using MEC-1 cell–derived exosomes, we confirmed the presence of CD20 on vesicles by immunoelectron microscopy (Fig. 1F) and flow cytometry (Fig. 1G). Assuming that extracellular CD20 is mainly associated with vesicles, we quantified CD20 in CLL- and healthy donor–derived plasma samples and observed significantly higher levels in CLL patients ($P = 0.008$; Fig. 1H).

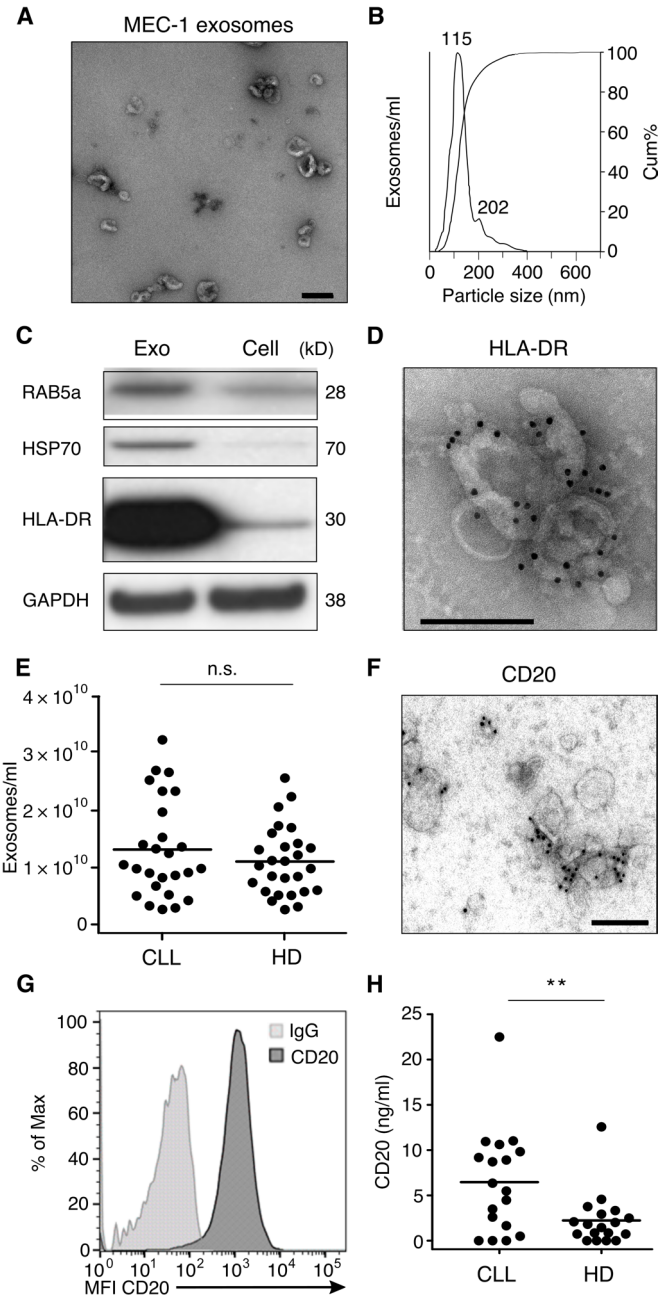

Fig. 1. Characterization and quantification of CLL-derived exosomes. (**A** to **D**) Characterization of MEC-1 exosomes (Exo). (A) Transmission electron microscopy (representative of seven independent measurements). Scale bar, 200 nm. (B) Size profile by NTA (representative of five independent measurements). %cum, cumulative percentage. (C) Western blot analysis of RAB5a, HSP70, and HLA-DR for MEC-1 Exo and parental cells (representative of two to three independent experiments). (D) Immunogold electron microscopy for HLA-DR (representative of six independent experiments). Scale bar, 200 nm. (**E**) Absolute Exo counts in plasma of CLL patients ($n = 26$) and healthy donors (HD; $n = 27$) acquired by NTA. $P = 0.30$. n.s., not significant. (**F**) CD20 detection on MEC-1 Exo via immunogold electron microscopy. Scale bar, 200 nm. (**G**) Flow cytometry analysis of CD20 on MEC-1 Exo coupled to latex beads (representative of three independent experiments). IgG, immunoglobulin G. (**H**) Quantification of CD20 in CLL ($n = 18$) and HD ($n = 18$) plasma via ELISA. $^{**}P = 0.008$. For (E) and (H), horizontal lines represent mean values; *P* values were determined by unpaired *t* test.

We further identified a similar pattern of increased CD20 levels in plasma exosome preparations of patients compared with healthy donors (fig. S1G). Although no correlation of CD20 with clinical parameters was detected (fig. S1H), elevated CD20 plasma levels indicated an enrichment of B cell–derived exosomes in CLL, which are most likely derived from the leukemic cells.

The noncoding Y RNA hY4 is enriched in CLL-derived exosomes

Comparison of RNA profiles of MEC-1 exosomes and respective parental cells showed an enrichment of small RNA in exosomes (Fig. 2A). Therefore, we conducted small RNA (<200 nt) sequencing of MEC-1– and CLL plasma–derived exosomes. Bioinformatic analysis of sequencing data revealed a notable difference in RNA composition of exosomes and cells, allowing a distinction of exosomal and cellular samples (Fig. 2, B to D, and tables S3 to S5). rRNA was the most abundant RNA species in exosomes, with all rRNA sequences covered (Fig. 2, D and E, and table S3), whereas small nucleolar RNA represented the most abundant RNA species in cells and showed much lower abundance in exosomes (Fig. 2, D and E). miRNA profiles were similar for exosomes and cells, with the top-expressed miRNAs miR-148a, miR-21, and miR-155 known to be abundant and prognostically relevant in CLL (Fig. 2F and table S3) (*29*, *30*).

Y RNAs were identified as the most significantly enriched RNA species in MEC-1 exosomes compared with cells (Fig. 2C) that was highly abundant both in primary CLL plasma–derived and MEC-1 exosomes (Fig. 2D and tables S3 and S5). hY4 and putative pseudogenes thereof accounted for 5.4 and 11.1% of total reads in CLL plasma and MEC-1 exosomes, respectively (Fig. 2, E and G, and table S3). This is notably different from the cellular Y RNA distribution, where hY4 and hY1 are rare but present at similar levels (0.6% of total reads; Fig. 2G and table S3). Most hY4 reads aligned to the 5′ region of the *RNY4* gene (Fig. 2H).

Validation of sequencing results by Northern blot analysis confirmed the presence of both full-length hY4 and a previously described 31-nt 5′ fragment hY4 (*31*) in MEC-1 cells and exosomes, with enrichment of the 5′ fragment in exosomes (Fig. 3A). Full-length and 5′ fragment hY4 were also elevated in plasma exosomes of CLL patients compared with healthy donors, which is most likely due to the enrichment of CLL cell–derived exosomes in patients' plasma (Fig. 3A). A direct comparison by Northern blot of total peripheral blood mononuclear cells (PBMCs) from CLL or healthy donor blood samples showed an enrichment of hY4 in CLL PBMC preparations (Fig. 3B). However, no difference in hY4 levels was detectable when isolated B cells of CLL patients or healthy donors were compared, suggesting that both malignant and normal B cells comparably express hY4 and are the main source of hY4 in blood (Fig. 3C). Beyond CLL, we detected hY4 in cells and exosomes of U87 glioma and MDA-MB-231 breast carcinoma cell lines, as well as in HS-5 bone marrow stromal cells and HMEC-1 endothelial cells (fig. S2, A to C), which is in line with the described ubiquitous expression of Y RNA in normal tissues and tumors (*32*–*34*).

CLL-derived exosome uptake triggers cytokine release and PD-L1 expression in monocytes

In previous studies, myeloid cells were identified to be the main target cells of MEC-1 exosomes (*26*). We therefore analyzed uptake of CLL-derived exosomes and induction of disease-associated changes in monocytes and macrophages. To this end, MEC-1 exosomes labeled with the green fluorescent membrane dye PKH67 were added to murine macrophage J774 cells. Uptake could be observed as early as 1 hour after treatment, with exosomes accumulating in recipient cells over time (Fig. 4, A and B). Counterstaining with anti-human HLA-DR and phalloidin demonstrated the capability of cargo transfer by exosomes and their intracellular localization in recipient cells (Fig. 4C and fig. S3A). Exosome uptake was confirmed with plasma-derived exosomes using human primary monocytes and in vitro–differentiated human primary macrophages as recipient cells (fig. S3, B and C). Treatment of primary monocytes with MEC-1 exosomes resulted in an average of 85% cells being positive for PKH67-labeled exosomes after 8 hours (Fig. 4D). Thereby, uptake of CLL-derived exosomes was not primarily mediated by cell surface heparan sulfate proteoglycans, as described previously (*26*), because previous incubation of exosomes with heparin did not efficiently block uptake (fig. S3D).

Because plasma exosome preparations contain not only tumor-derived vesicles but also a mixture of exosomes produced by many cell types including platelets, MEC-1 exosomes were used as a model system to analyze cellular responses in monocytes. Immunophenotyping of monocytes after overnight treatment with MEC-1 exosomes showed an increased expression of PD-L1 and a decrease in C-C motif chemokine receptor 2 (CCR2) expression levels (Fig. 4, E and F)—features of myeloid cells that have been described for CLL (*5*, *7*). In addition, secretion of C-C motif chemokine ligand 2 (CCL2) and CCL4 and interleukin-6 (IL-6) was observed upon MEC-1 exosome treatment (Fig. 4G), which is in line with induced nuclear factor κB (NF-κB) activity (fig. S3E). We did not detect PD-L1 or the abovementioned cytokines in the proteome of exosomes (table S2) or by flow cytometry on their surface (fig. S3F), and exosomes did not show chemotactic activity for monocytes (fig. S3G), suggesting that PD-L1 expression and cytokine secretion were induced in monocytes upon exosome treatment, rather than presented or transferred to monocytes via CLL-derived exosomes. Treatment with plasma-derived exosomes also triggered comparable alterations in PD-L1 and CCR2 expression (Fig. 4, H and I).

Uptake of hY4 induces cytokine secretion and immunosuppressive molecules in monocytes, mirroring the CLL microenvironment

To assess the involvement of exosomal RNA in observed phenotypic changes, full-length (96 nt) and 5′ fragment (31 nt) hY4 were synthesized and delivered to primary monocytes using Effectene lipoplexes. The amount of added hY4 was adjusted to reflect its abundance in MEC-1 exosomes as outlined in the Supplementary Materials. Transfer of RNA, as monitored by flow cytometry, resulted in 82.1% positive cells upon treatment with Alexa 488–coupled 5′ fragment hY4 (Fig. 5A). Confocal microscopy revealed an accumulation of this labeled hY4 fragment in late endosomes/lysosomes (Fig. 5B).

To evaluate the impact of hY4 on transcriptional changes in monocytes, we performed reverse transcription polymerase chain reaction (RT-PCR) arrays for 84 genes involved in cancer inflammation and immunity cross-talk. Monocytes were treated with Effectene alone (control), 5′ fragment hY4, or full-length hY4 packaged in Effectene. A strong induction of gene expression upon delivery of hY4 compared with control cells was observed for most of the genes, with 48 significantly different genes showing at least twofold up-regulation in full-length hY4–treated monocytes (Fig. 5C; fig. S4, A and B; and table S6). Overall, a stronger regulatory effect for full-length hY4 compared with 5′ fragment hY4 was observed (Fig. 5D). Among the most up-regulated

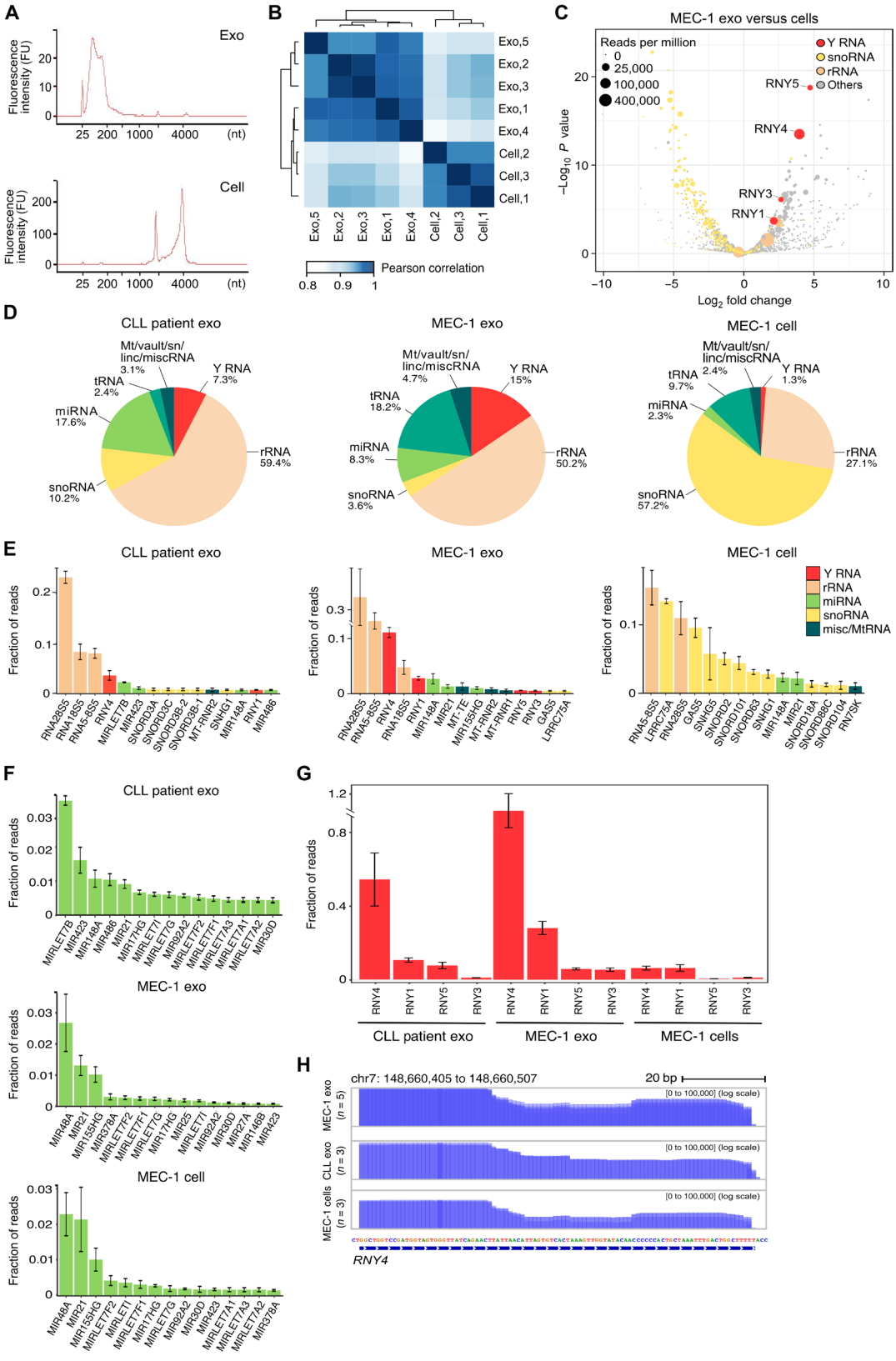

Fig. 2. Small RNA sequencing of CLL plasma–derived exosomes and MEC-1 exosomes and cells. (**A**) Whole-RNA profiles of MEC-1 exosomes (Exo) and cells obtained by Agilent 2100 Bioanalyzer (representative of three independent measurements). FU, fluorescence units. (**B** to **H**) Sequencing of small RNA (<200 nt) of CLL plasma–derived Exo (n = 3), MEC-1 Exo (n = 5), and MEC-1 cells (n = 3). (B) Heat map showing Pearson correlations of the top 1000 most abundant small RNA transcripts of MEC-1 Exo and cells. (C) Volcano plot showing the differential abundance of noncoding RNA transcripts in MEC-1 Exo compared with cells. Bubble size corresponds to average read counts per 1 million reads; P values were calculated by DESeq2 and corrected for multiple testing using the Benjamini-Hochberg method. snoRNA, small nucleolar RNA. (D) Read distribution of noncoding RNA species for CLL plasma–derived Exo and MEC-1 Exo and cells. Mt/vault/sn/linc/misc RNA, mitochondrial/vault/small nuclear/long intergenic noncoding/miscellaneous RNA. (E) Top 15 abundant RNA transcripts. (F) Top 15 abundant miRNA transcripts. (G) Read distribution of four human Y RNAs. For (E) to (G), error bars represent the SEM. (H) Coverage plots of full-length hY4 transcript were visualized by Integrative Genomic Viewer; individual tracks from replicates were merged and visualized with the overlay option. Y axis is shown in log scale.

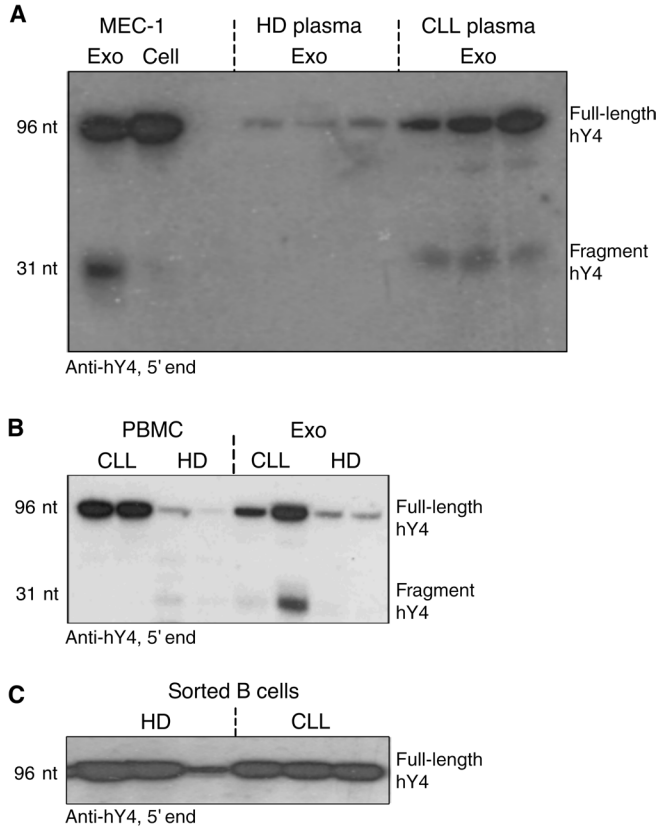

Fig. 3. Northern blot analysis of hY4 in CLL-derived exosomes and cells. Full-length (hY4 96 nt) and 5′ fragment hY4 (hY4 31 nt) were detected using an antisense DNA oligonucleotide probe against the 5′ end of hY4. Sample loading per lane: (**A**) 150 ng of RNA of MEC-1 exosomes (Exo) and cells (representative of five independent measurements), as well as total exosomal RNA of 3 ml of healthy donor (HD) and CLL plasma each; (**B**) 200 pg of RNA of PBMCs, as well as total exosomal RNA of 3 ml of HD and CLL plasma each; and (**C**) 150 ng of RNA of CD19-sorted B cells of three HD and three CLL patients.

genes were chemokines [including *CCL2*, *CCL4*, *CCL5*, C-X-C motif chemokine ligand 9 (*CXCL9*), *CXCL10*, and *CXCL11*], proinflammatory genes [such as *IL6*, *IL12A*, and *TNF* (tumor necrosis factor)], and also immunosuppressive factors [such as *CD274* (also known as PD-L1), *IDO1*, and *PDCD1* (also known as programmed cell death protein 1, PD-1)] (Fig. 5C and table S6). Most of these genes are known as interferon response genes or genes regulated via signal transducer and activator of transcription (STAT) and NF-κB signaling. Down-regulated genes mostly included chemokine receptors such as *CCR2* and *CXCR4* (Fig. 5C and table S6).

For validation, cytokine release in monocytes was monitored upon delivery of full-length and 5′ fragment hY4, as well as upon treatment with two miRNAs, miR-21 and miR-15a. Both miRNAs are prognostically and functionally relevant in CLL but are opposing regarding their regulation in CLL and their putative role in exosomes (*30*, *35*, *36*). miR-21 is up-regulated in CLL and has been shown to mediate cytokine release in monocytes upon exosomal delivery. In contrast, miR-15a is absent or down-regulated in CLL and has not been detected in CLL-derived exosomes. Full-length hY4 showed a pronounced higher potency regarding secretion of CCL2, CCL3, CCL4, CXCL10, and IL-6, when compared with any other delivered RNAs (Fig. 5E). In addition, increased expression of PD-L1 upon treatment with full-length hY4 was confirmed by flow cytometry, again showing lack of or reduced effects for any other delivered RNAs (Fig. 5F). For CCR2, baseline expression varied between monocyte preparations, but if expressed, CCR2 was readily down-regulated upon treatment with full-length hY4 and, to some extent, with miR-21 (Fig. 5G). A direct comparison of full-length and fragment hY4 further showed a concentration-dependent activity for both RNAs and confirmed a higher potency of full-length hY4 for the described responses in monocytes (fig. S4, C to E). Last, we also confirmed the ability of RNA isolated from MEC-1 exosomes to induce up-regulation of PD-L1, IL-6, and CCL4 and down-regulation of CCR2 (Fig. 5H).

To address the relevance of our observations for CLL pathogenesis, we performed a cytokine array with serum samples of 11 CLL patients and 5 healthy donors and compared the results with transcriptional changes induced by hY4 in monocytes shown in Fig. 5C. In total, 15 of 20 cytokines that were measured by both assays and were elevated in CLL serum were also induced by hY4 treatment (Fig. 5I and table S7). Among them were candidate cytokines including IL-6, CCL4, CXCL10, and CCL2, suggesting that hY4-induced responses in monocytes contribute to the inflammatory milieu in CLL. Together with the enhanced expression of PD-L1 that was observed on monocytes in human and murine CLL (*7*), hY4-induced changes reflect multiple CLL-associated phenotypes.

The Y RNA hY4 mediates downstream effects via TLR7 signaling

Our previous work identified TLR signaling as a major pathway activated in CLL cocultures (*4*). Because we observed intracellular accumulation of hY4 in acidified endosomes, we hypothesized that hY4 may act as a ligand for endosomal TLR7 or TLR8, both of which recognize single-stranded RNA (*37*, *38*). TLR8 has been shown to have reduced functionality in mice; therefore, we used *Tlr7* knockout (KO) mice to test this hypothesis. *Mavs* KO mice were further included in this study, because mitochondrial antiviral signaling protein (MAVS) mediates signaling downstream of the cytoplasmic pattern recognition receptor retinoic acid–inducible gene I (RIG-I), which has been previously reported to recognize exosomal RNA in breast cancer cells (*39*). Bone marrow–derived myeloid cells from *Tlr7* KO and *Mavs* KO mice as well as corresponding wild-type mice were isolated and treated with hY4, as described above. Induction of cytokine secretion, up-regulation of PD-L1, and down-regulation of CCR2 expression upon treatment with hY4 were observed in myeloid cells from wild-type or *Mavs* KO mice but were completely abolished in cells that lack TLR7, indicating that hY4-induced responses were dependent on TLR7 (Fig. 6, A and B, and fig. S5, A to C). Stimulation of TLR4 using lipopolysaccharide (LPS) resulted in similar responses in all samples, confirming a comparable inflammatory potential of the cells.

Chloroquine treatment decreases exosomal effects in monocytes and inhibits CLL development in mice

To evaluate the relevance of TLR7/8 activity for CLL development, we used chloroquine, which inhibits acidification of endosomes/lysosomes and therefore endosomal TLR activity (*40*), in vitro and in the Eμ-TCL1 mouse model of CLL. Pretreatment of monocytes with chloroquine impaired cytokine release and PD-L1 expression upon delivery of full-length hY4 or CLL-derived exosomes, confirming the relevance of endosomal TLR activity in exosomal effects (Fig. 6C and fig. S5D). Chloroquine treatment of CLL-bearing mice (after adoptive transfer of

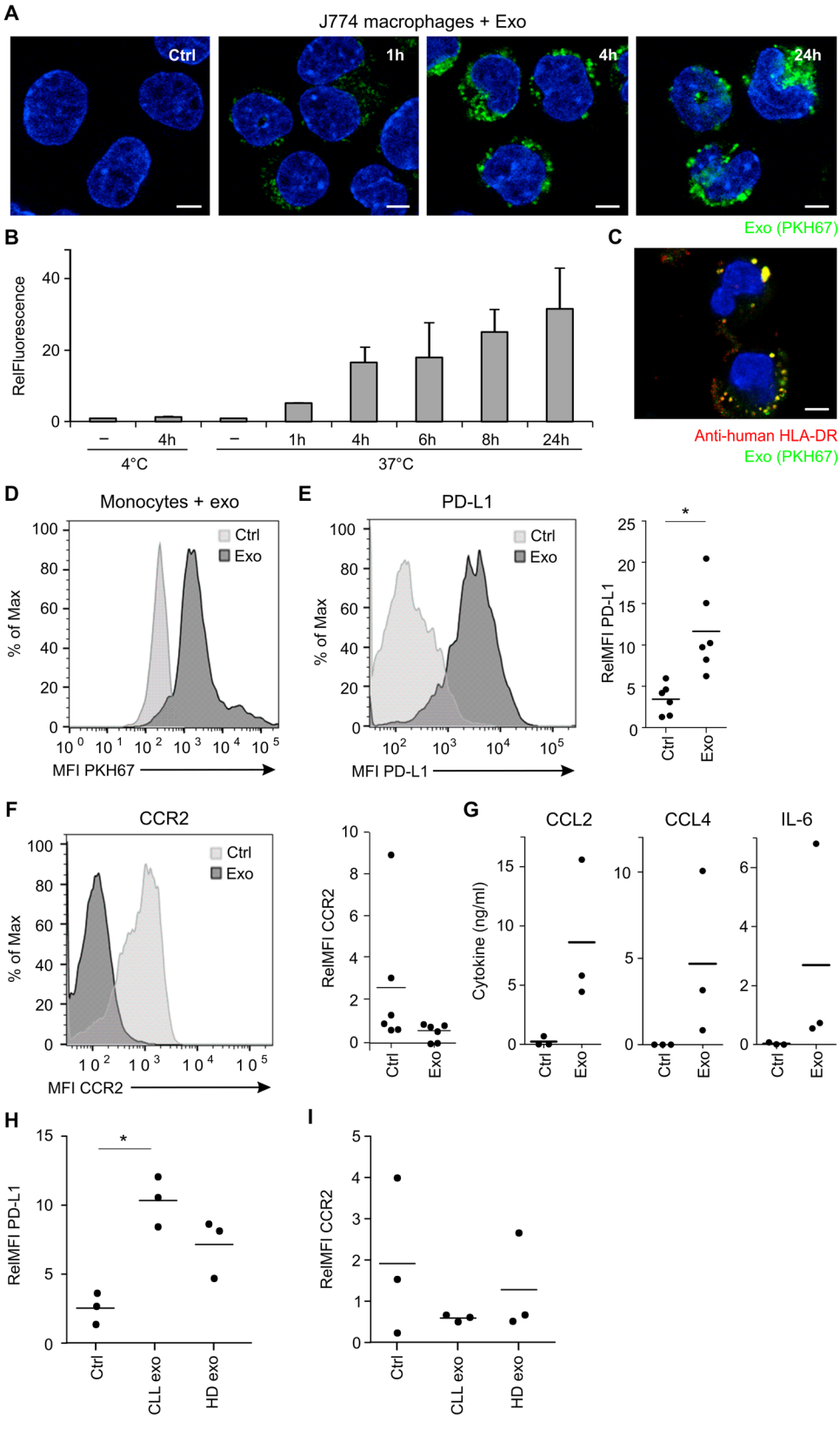

Fig. 4. Uptake of MEC-1 exosomes in myeloid cells, induction of PD-L1 expression, and cytokine release. (**A** to **C**) J774 cells were treated with 10 μg of PKH67-labeled MEC-1 exosomes (Exo). (A) Confocal microscopy (representative of four independent experiments). Blue, nuclear staining with 4′,6-diamidino-2-phenylindole; green, membrane labeling of Exo with PKH67. 1h, 1 hour. Scale bars, 5 μm. (B) Quantification of uptake shown as mean fold changes (±SD) of Exo treated at 4° or 37°C, over untreated J774 cells at 37°C ($n = 2$). RelFluorescence, relative fluorescence. (C) Costaining of human HLA-DR (red) and PKH67$^+$ MEC-1 Exo. Scale bar, 5 μm. (**D**) Uptake of 5 μg of PKH67-labeled MEC-1 Exo by human primary monocytes was analyzed by flow cytometry after 8 hours of Exo treatment (representative of three independent experiments). (**E** and **F**) Expression of PD-L1 (E) and CCR2 (F) in monocytes after 8 hours of treatment with 3 to 5 μg of MEC-1 Exo was analyzed by flow cytometry. Relative median fluorescence intensity (MFI) (RelMFI) was normalized to isotype control ($n = 6$ each) (right); representative histogram (left). (**G**) Cytokine concentrations in cell culture supernatant of monocytes after 8 hours of treatment with 5 μg of MEC-1 Exo were measured by ELISA (CCL2) and cytometric bead array (CCL4 and IL-6) ($n = 3$). (**H** and **I**) Expression of PD-L1 (H) and CCR2 (I) in monocytes after 8 hours of treatment with 5 μg of CLL or healthy donor (HD) plasma–derived Exo ($n = 3$) was analyzed by flow cytometry; RelMFI was normalized to isotype control. For (A) and (D) to (I), Ctrl denotes phosphate-buffered saline. For (E) to (I), mean values are depicted by horizontal lines. *P* values were determined by paired *t* test. **P* = 0.02 (E); **P* = 0.01 (H).

malignant splenocytes from *E*μ-TCL1 mice) decreased leukemia development, as shown by reduced absolute numbers of malignant cells in the blood and spleen as well as lower spleen weights of the animals after treatment (Fig. 6, D to F). Together, this suggests that exosomal RNA–mediated activation of TLR7/8 signaling contributes to CLL development, by triggering a supportive tumor microenvironment.

DISCUSSION

In the current study, we have identified the Y RNA hY4 as an abundant transcript in CLL-derived exosomes and demonstrated that it has a central function in generating a tumor-supportive microenvironment. Enrichment of small RNAs with a similar size distribution as in our analyses was observed in EV preparations before (*18*, *19*). RNA sequencing approaches revealed the

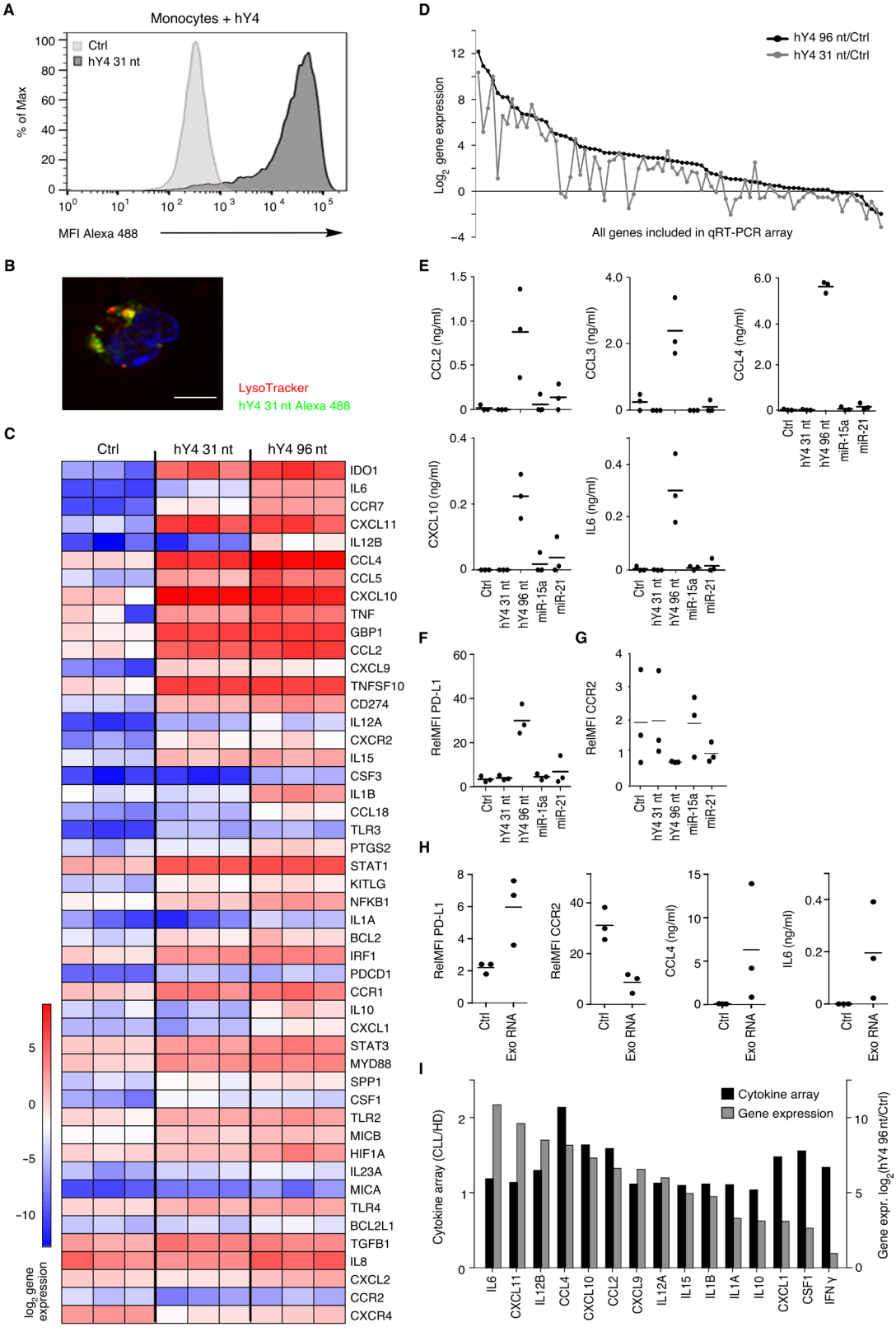

Fig. 5. Response of monocytes to hY4 delivery and cytokine levels in CLL serum. Human primary monocytes were treated with Effectene-packaged RNA for 8 hours. (**A** and **B**) Uptake of 50 nM Alexa 488–coupled hY4 fragment (hY4 31 nt) was analyzed by flow cytometry (A) and confocal microscopy (B) (representative of three independent experiments each). Blue, nuclear staining with Hoechst 33342; red, staining of acidified endosomes and lysosomes with LysoTracker DND-99; green, Alexa 488–coupled hY4 fragment. Scale bar, 10 μm. (**C** and **D**) Gene expression data of primary human monocytes treated with Effectene alone (Ctrl), 50 nM hY4 5′ fragment (hY4 31 nt) or 50 nM full-length hY4 (hY4 96 nt) were obtained by quantitative RT-PCR array (n = 3 each). P values were determined by moderated t test via empirical Bayes method and adjusted using the method of Benjamini and Hochberg to control the false discovery rate. (C) Heat map of $\log_2$ gene expression data of significantly deregulated genes with at least twofold change, sorted according to fold change of hY4 96 nt over Ctrl. (D) Comparison of expression levels for all analyzed genes. (**E**) Cytokine concentrations in cell culture supernatant of monocytes treated with 50 nM RNA were analyzed by ELISA (CCL2 and CCL3) and cytometric bead array (CCL4, CXCL10, and IL-6) (n = 3). (**F** and **G**) Expression of PD-L1 (F) and CCR2 (G) in monocytes treated with 50 nM RNA was analyzed by flow cytometry (n = 3). Relative median fluorescence intensity (RelMFI) was normalized to isotype control is depicted. (**H**) Expression of PD-L1 and CCR2, as well as cell culture cytokine concentrations upon monocyte treatment with 600 ng of Effectene-packaged MEC-1 exosomal RNA (Exo RNA), was analyzed by flow cytometry and cytometric bead array, respectively (n = 3). For (E) to (H), mean values are depicted by horizontal lines. P values were determined by paired t test. $^*P < 0.05$; $^{***}P < 0.001$. (**I**) Comparison of serum cytokine ratios of 11 CLL patients versus 5 healthy donors (HD) analyzed by cytokine array (black bars), and gene expression data provided in (B) (gray bars show $\log_2$ fold change of hY4 96 nt versus Ctrl). Cytokines that are transcriptionally induced by hY4 in monocytes and elevated in CLL plasma are depicted. For (A) to (H), Ctrl denotes Effectene alone.

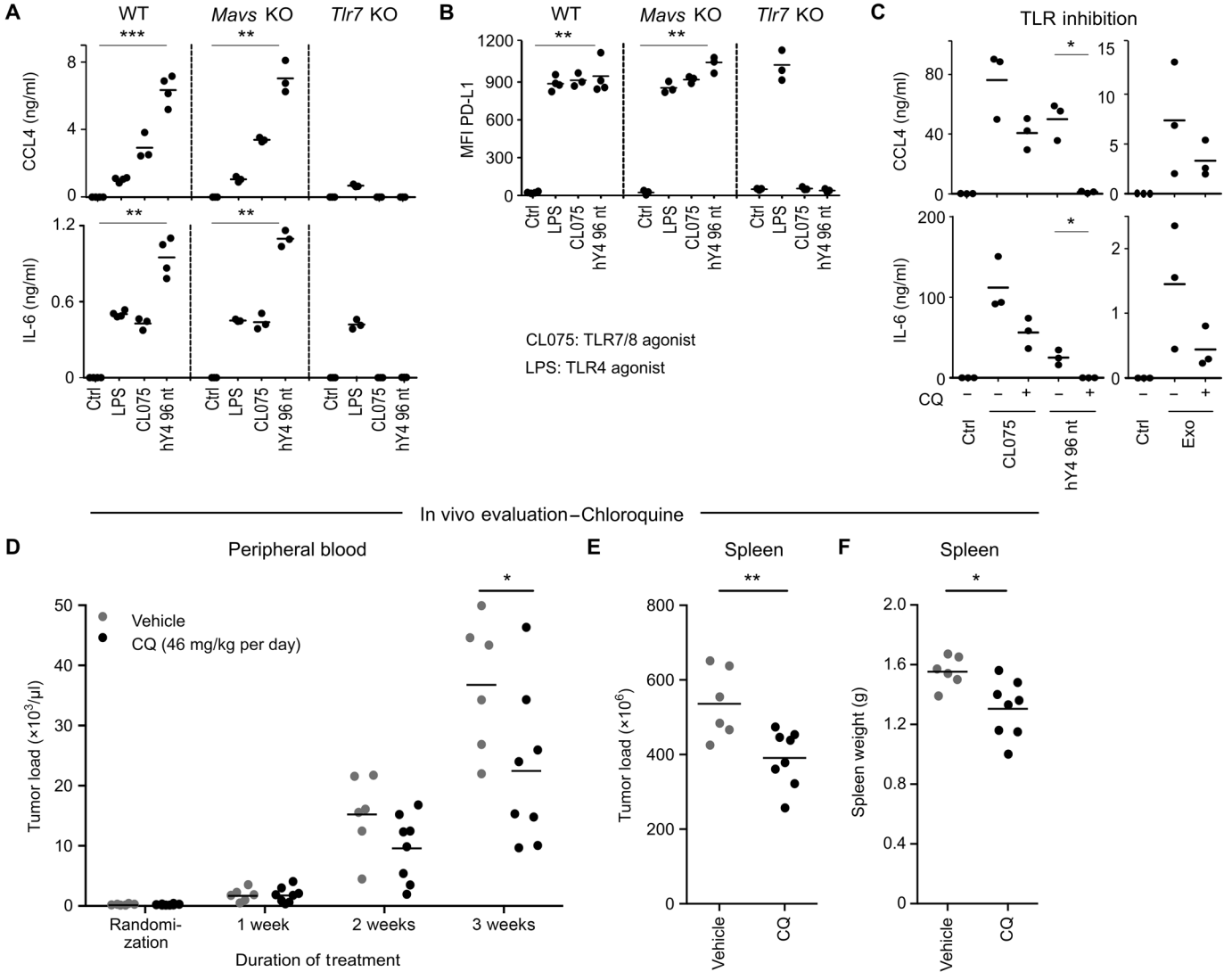

Fig. 6. Role of TLR signaling in hY4-induced changes and effects of TLR inhibition. (**A** and **B**) Response of bone marrow–derived myeloid cells of wild-type (WT), *Mavs* KO, and *Tlr7* KO mice ($n = 3$ to 4 each) 8 hours after treatment with 50 nM Effectene-packaged full-length hY4 (hY4 96 nt) or the TLR agonist LPS or CL075. (A) Cytokine concentrations in culture supernatant were analyzed by cytometric bead array (CCL4) and ELISA (IL-6). (**B**) PD-L1 expression measured by flow cytometry. (**C**) Monocytes were pretreated with 50 µM chloroquine (CQ) for 30 min to inhibit TLR signaling, before treatment with 50 nM Effectene-packaged full-length hY4 (hY4 96 nt) (left) or 10 µg of MEC-1 exosomes (Exo) (right). Cytokine concentrations in cell culture supernatant were measured by cytometric bead array after 8 hours ($n = 3$). (A to C) Ctrl, Effectene alone; CL075 and LPS, Effectene + CL075 (3 µg/ml) (TLR7/8 agonist) or + LPS (10 ng/ml) (TLR4 agonist). (**D** to **F**) Therapeutic targeting of TLR signaling by CQ treatment in vivo. C57BL/6 mice were transplanted with 1.5×10^7 splenocytes from leukemic *E*µ-TCL1 mice and randomized to treatment, with vehicle or CQ (46 mg/kg per day) added to drinking water. (D) Tumor load in blood at indicated time points of treatment as absolute counts of circulating $CD5^+CD19^+$ CLL cells was determined by flow cytometry. (E) Tumor load in spleen after 3.5 weeks of treatment as absolute counts of $CD5^+CD19^+$ CLL cells was determined by flow cytometry (F) and spleen weight. For (A) to (F), mean values are depicted by horizontal lines. For (A) to (C), *P* values were determined by paired *t* test. For (D) to (F), *P* values were determined by unpaired *t* test. $^*P < 0.05$; $^{**}P < 0.01$; $^{***}P < 0.001$.

presence of Y RNAs or their 5′ fragments in exosomes of cancer and noncancer cells (*19*, *32*, *41*–*43*). Our sequencing data revealed an enrichment of hY4 in exosomes, with four- and fivefold higher levels compared with hY1 in MEC-1– and CLL plasma–derived exosomes, respectively, whereas MEC-1 cells contained overall much lower but roughly equal levels of these two Y RNAs. This is in line with a report by Tosar *et al.* (*32*) who observed in breast cancer cells and their derived exosomes that >85% of Y RNA–derived reads corresponded to hY4. Y RNAs were further shown to represent a major small noncoding RNA species in exosomes derived from lymphoblastoid and lymphoma B cell lines, and again, a notable enrichment of hY4 over other Y RNAs in exosomes was observed (*41*). We also detected hY4 in nonmalignant cell types, including fibroblasts, endothelial cells, and B cells of healthy individuals, confirming a ubiquitous expression of this Y RNA (*33*). Because exosome secretion in B cells is induced upon B cell receptor activation, the observed hY4-mediated effects in monocytes might reflect physiological activities of normal immune responses. This is supported by our observation that healthy donor plasma exosomes induced a partial response in terms of PD-L1 and CCR2 expression and cytokine secretion in monocytes. In CLL, malignant B cells and their derived exosomes accumulate

in lymph nodes and blood, resulting in a chronic stimulation and activation of myeloid cells. In contrast, the physiological activity of B cell–derived exosomes during infections is most likely more controlled in magnitude and duration.

We have also identified signaling via endosomal TLR7 as the underlying mechanism of exosomal effects in monocytes and show that exosomal RNAs display a species- and concentration-dependent potency in inducing these effects. In accordance, exosomal RNAs were reported to trigger pattern recognition receptor signaling in recipient cells, either via activation of cytoplasmic RIG-I as shown by Boelens *et al*. (*39*) in breast cancer cells or via endosomal TLR7 stimulation by miR-21 in macrophages (*35*), which was associated with increased tumor growth and metastasis.

The specificity of hY4-mediated activation of TLR7 signaling remains elusive. Characterization of potential binding motifs within hY4 for TLR7, which most likely depend on the RNA sequence, respective secondary structures, and posttranscriptional modifications (*38*, *44*), needs to be addressed in future investigations. The observed enrichment of hY4 in exosomes implies a specific sorting mechanism that is also not understood so far. Sorting via 3′ end polyU (polyuridylic acid) motifs (*41*) might be of relevance given that Y RNAs and other noncoding RNAs present in exosomes are RNA polymerase III transcripts with a characteristic polyT (polythymidylic acid) sequence at the 3′ end of the gene (*45*). However, this does not explain the overall elevated abundance of hY4 over other Y RNAs in exosomes.

Tumor exosomes have been linked to inflammatory processes as well as several aspects of tumor pathobiology (*46*, *47*). In particular, CLL-derived exosomes were shown to induce the generation of cancer-associated fibroblasts, which display an inflammatory and proangiogenic phenotype and were detected in patients' lymph nodes (*26*). Subcutaneous coinjections of MEC-1 cells and exosomes further revealed a tumor growth–promoting effect of CLL-derived exosomes. A recent report showed a tremendous increase of exosome release by CLL cells upon B cell receptor activation, which implies a central role of CLL-derived exosomes in the microenvironment of secondary lymphoid tissues, the sites of B cell activation (*24*). Monocytes and macrophages at these sites are skewed toward protumorigenic phenotypes, including increased expression of immunosuppressive proteins such as PD-L1, as well as enhanced secretion of inflammatory cytokines that accumulate in the serum of patients (*4*, *7*). The results of our study suggest that CLL-derived exosomes and their contained Y RNA trigger these local and systemic tumor-supportive alterations.

RNY4 does not exist in mice, and therefore, the *E*μ-TCL1 mouse model of CLL cannot be used to address the role of this RNA in vivo. Other murine Y RNAs might be involved in disease development in these mice, but considering the small amounts of blood plasma that can be obtained, functional studies with murine exosomes are very limited. Instead, we used *E*μ-TCL1 mice to therapeutically target TLR activity with chloroquine, which slowed down disease development. This might be due to alterations in the microenvironment but also due to the direct effects on the malignant cells, as observed in vitro (*48*). Results of a small clinical trial of hydroxychloroquine treatment in CLL over 1 year showed that 12 of 22 treated patients presented with a fall in absolute numbers of malignant cells in the blood and that 7 further patients presented with stable disease throughout the trial (*49*). This encouraging result, together with our recent finding that immune checkpoint blockade using anti–PD-L1 antibodies successfully controls CLL development in mice (*8*), paves the way for therapeutic interventions targeting the CLL microenvironment. As we show here that PD-L1 expression is induced in monocytes by CLL-derived exosomes or exosomal hY4, rational combination therapies that include exosomal targets or their triggered responses, such as TLR signaling, have to be considered as novel treatment approaches for CLL. Last, because Y RNAs were detected in tumor-derived exosomes of several cancers, and tumor-associated chronic inflammation and up-regulated PD-L1 expression are frequently observed, our findings are likely of relevance in cancer beyond CLL.

MATERIALS AND METHODS

Study design

Animal studies were conducted under a protocol approved by the local animal experimental ethics committee (Regierungspräsidium Karlsruhe, Germany) and according to their guidelines. Group size of the two treatment arms was determined on the basis of expected variances within the groups of 20% and was determined to be able to prove a difference between the groups of at least 25%. Mice were randomized before treatment on the basis of tumor burden, which was determined as the absolute number of $CD5^+CD19^+$ cells in the blood analyzed via flow cytometry. Mice were euthanized after 3.5 weeks of treatment, when vehicle-treated mice achieved a fully leukemic state.

Exosome isolation, quantification, and characterization

Culture supernatant of MEC-1 cells as well as blood plasma samples were used for exosome isolation as previously described (*27*). Quantification of exosomes was performed via NTA using NanoSight LM10 equipped with a 405-nm laser (Malvern Instruments, Worcestershire, UK), CD81 ExoELISA (System Biosciences, Palo Alto, CA, USA), and human B lymphocyte antigen (CD20) ELISA kit (Cusabio Biotech, College Park, MD, USA). Exosome morphology was assessed by transmission electron microscopy as previously described (*27*). Western blot analysis of MEC-1 exosomes was performed as described in the Supplementary Materials. Evaluation of CD20 surface expression was assessed by flow cytometry after coupling MEC-1 exosomes to 4-μm aldehyde/sulfate latex beads (Thermo Fisher Scientific).

Mass spectrometry of blood plasma–derived exosomes

Proteome profiling was performed as previously described (*27*). Mass spectrometry data were obtained using a nanoACQUITY UPLC system (Waters, Eschborn, Germany) and analyzed with the MaxQuant open source software, as detailed in the Supplementary Materials.

RNA sequencing of CLL-derived exosomes

Exosomal RNA for sequencing was isolated using miRNeasy Micro Kit (Qiagen, Hilden, Germany), following the manufacturer's instructions for the isolation of small RNA (<200 nt). Sequencing libraries were prepared using NEBNext Multiplex Small RNA Prep Set for Illumina, and 51–base pair single-end sequencing was performed using HiSeq version 4 platform (Illumina, San Diego, CA, USA). Analysis of sequencing data was performed as described in the Supplementary Materials.

Northern blot analysis

A 32-nt antisense oligonucleotide probe against the 5′ end of hY4 (5′-AGTTCTGATAACCCA CTACCATCGGACCAGCC-3′) (*31*) labeled with 20 pmol of [γ^{32}-P]adenosine 5′-triphosphate was used for Northern blot analysis, as described in the Supplementary Materials.

Uptake studies
Uptake of PKH67-labeled exosomes or Alexa 488–labeled hY4 by monocytes or macrophages was analyzed by flow cytometry or confocal microscopy, as described in the Supplementary Materials.

Gene expression analysis of hY4-treated monocytes
Monocytes treated with Effectene alone (control), 50 nM hY4 fragment (31 nt), or 50 nM hY4 (96 nt), both packaged in Effectene, were analyzed using the Cancer Inflammation and Immunity Crosstalk RT^2 Profiler Array (Qiagen), according to the manufacturer's instructions, and heat maps of $\log_2$ fold changes of $2^{-\Delta\Delta Ct}$ values were generated.

Functional assays
Human monocytes or murine bone marrow–derived myeloid cells were treated with exosomes, synthetic RNA oligonucleotides, exosomal RNA, TLR7/8 agonist CL075, or TLR4 agonist LPS. Where indicated, 50 μM chloroquine was added 30 min before stimulation to block TLR signaling. Changes in PD-L1 and CCR2 expression were evaluated by flow cytometry. Alterations in cytokine levels were assessed via cytometric bead arrays or ELISA kits, as described in the Supplementary Materials.

Serum cytokine array
Serum cytokine levels were evaluated by human cytokine arrays [RayBio Glass Slide-based Antibody Arrays (G-Series), RayBiotech, Norcross, GA, USA], according to the manufacturer's instructions. Axon GenePix 4000A Microarray Scanner and GenePix Pro 6.0 software were used for data analysis.

Chloroquine treatment of mice
Adoptive transfer of *E*μ-TCL1 leukemia was performed as described previously (*7*). Mice were randomized on the basis of tumor burden to treatment with β-cyclodextrin (0.01 g/ml)–fortified and glucose (0.015 g/ml)–fortified drinking water (vehicle) or with chloroquine (0.288 mg/ml) in vehicle (46 mg/kg per day) for 3.5 weeks, after which mice were sacrificed. Spleens were weighed, and tumor load in spleen was determined as the absolute number of CD5$^+$CD19$^+$ cells via flow cytometry.

Statistics
Details of statistical analyses are provided in the Supplementary Materials.

Study approval
All investigations involving experiments on human material (blood cells and plasma) were approved by the local ethics committees in Essen, Heidelberg, and Ulm, and participants have given written informed consent in accordance with the Declaration of Helsinki.

SUPPLEMENTARY MATERIALS
immunology.sciencemag.org/cgi/content/full/2/13/eaah5509/DC1
Materials and Methods
Fig. S1. Plasma exosome quantification and correlation with clinical parameters.
Fig. S2. Northern blot analysis of hY4 in non-CLL exosomes and cells.
Fig. S3. Exosome uptake and triggered response in myeloid cells.
Fig. S4. hY4-induced gene expression changes and functional effects in monocytes.
Fig. S5. Relevance of TLR signaling in exosomal RNA–induced response.
Table S1. Patient information.
Table S2. Proteome of CLL and healthy donor plasma–derived exosomes.
Table S3. Small RNA sequencing data of CLL-derived exosomes and cells.
Table S4. Quality control data of small RNA sequencing libraries.
Table S5. Abundance of RNA species.
Table S6. Gene expression results of monocytes upon hY4 treatment.
Table S7. Comparison of serum cytokine levels with hY4-induced genes.
Table S8. Raw data.
References (*50*–*54*)

REFERENCES AND NOTES

1. D. Hanahan, R. A. Weinberg, Hallmarks of cancer: The next generation. *Cell* **144**, 646–674 (2011).
2. A. Mantovani, F. Marchesi, A. Malesci, L. Laghi, P. Allavena, Tumour-associated macrophages as treatment targets in oncology. *Nat. Rev. Clin. Oncol.* **14**, 399–416 (2017).
3. N. S. Nicholas, B. Apollonio, A. G. Ramsay, Tumor microenvironment (TME)-driven immune suppression in B cell malignancy. *Biochim. Biophys. Acta* **1863**, 471–482 (2016).
4. A. Schulz, G. Toedt, T. Zenz, S. Stilgenbauer, P. Lichter, M. Seiffert, Inflammatory cytokines and signaling pathways are associated with survival of primary chronic lymphocytic leukemia cells in vitro: A dominant role of CCL2. *Haematologica* **96**, 408–416 (2011).
5. R. Jitschin, M. Braun, M. Büttner, K. Dettmer-Wilde, J. Bricks, J. Berger, M. J. Eckart, S. W. Krause, P. J. Oefner, K. Le Blanc, A. Mackensen, D. Mougiakakos, CLL-cells induce IDO^{hi} CD14$^+$HLA-DR^{lo} myeloid-derived suppressor cells that inhibit T-cell responses and promote T_{Regs}. *Blood* **124**, 750–760 (2014).
6. R. Maffei, J. Bulgarelli, S. Fiorcari, L. Bertoncelli, S. Martinelli, C. Guarnotta, I. Castelli, S. Deaglio, G. Debbia, S. De Biasi, G. Bonacorsi, P. Zucchini, F. Narni, C. Tripodo, M. Luppi, A. Cossarizza, R. Marasca, The monocytic population in chronic lymphocytic leukemia shows altered composition and deregulation of genes involved in phagocytosis and inflammation. *Haematologica* **98**, 1115–1123 (2013).
7. B. S. Hanna, F. McClanahan, H. Yazdanparast, N. Zaborsky, V. Kalter, P. M. Rößner, A. Benner, C. Dürr, A. Egle, J. G. Gribben, P. Lichter, M. Seiffert, Depletion of CLL-associated patrolling monocytes and macrophages controls disease development and repairs immune dysfunction in vivo. *Leukemia* **30**, 570–579 (2016).
8. F. McClanahan, B. Hanna, S. Miller, A. J. Clear, P. Lichter, J. G. Gribben, M. Seiffert, PD-L1 checkpoint blockade prevents immune dysfunction and leukemia development in a mouse model of chronic lymphocytic leukemia. *Blood* **126**, 203–211 (2015).
9. S. El-Andaloussi, Y. Lee, S. Lakhal-Littleton, J. Li, Y. Seow, C. Gardiner, L. Alvarez-Erviti, I. L. Sargent, M. J. A. Wood, Exosome-mediated delivery of siRNA in vitro and in vivo. *Nat. Protoc.* **7**, 2112–2126 (2012).
10. P. D. Robbins, A. E. Morelli, Regulation of immune responses by extracellular vesicles. *Nat. Rev. Immunol.* **14**, 195–208 (2014).
11. C. Théry, M. Ostrowski, E. Segura, Membrane vesicles as conveyors of immune responses. *Nat. Rev. Immunol.* **9**, 581–593 (2009).
12. M. Colombo, G. Raposo, C. Théry, Biogenesis, secretion, and intercellular interactions of exosomes and other extracellular vesicles. *Annu. Rev. Cell Dev. Biol.* **30**, 255–289 (2014).
13. G. Raposo, W. Stoorvogel, Extracellular vesicles: Exosomes, microvesicles, and friends. *J. Cell Biol.* **200**, 373–383 (2013).
14. A. Zomer, C. Maynard, F. J. Verweij, A. Kamermans, R. Schäfer, E. Beerling, R. Michel Schiffelers, E. de Wit, J. Berenguer, S. I. J. Ellenbroek, T. Wurdinger, D. M. Pegtel, J. van Rheenen, In vivo imaging reveals extracellular vesicle-mediated phenocopying of metastatic behavior. *Cell* **161**, 1046–1057 (2015).
15. A. Montecalvo, A. T. Larregina, W. J. Shufesky, D. B. Stolz, M. L. G. Sullivan, J. M. Karlsson, C. J. Baty, G. A. Gibson, G. Erdos, Z. Wang, J. Milosevic, O. A. Tkacheva, S. J. Divito, R. Jordan, J. Lyons-Weiler, S. C. Watkins, A. E. Morelli, Mechanism of transfer of functional microRNAs between mouse dendritic cells via exosomes. *Blood* **119**, 756–766 (2012).
16. J. Skog, T. Würdinger, S. van Rijn, D. H. Meijer, L. Gainche, W. T. Curry Jr., B. S. Carter, A. M. Krichevsky, X. O. Breakefield, Glioblastoma microvesicles transport RNA and proteins that promote tumour growth and provide diagnostic biomarkers. *Nat. Cell Biol.* **10**, 1470–1476 (2008).
17. H. Valadi, K. Ekström, A. Bossios, M. Sjöstrand, J. J. Lee, J. O. Lötvall, Exosome-mediated transfer of mRNAs and microRNAs is a novel mechanism of genetic exchange between cells. *Nat. Cell Biol.* **9**, 654–659 (2007).
18. X. Huang, T. Yuan, M. Tschannen, Z. Sun, H. Jacob, M. Du, M. Liang, R. L. Dittmar, Y. Liu, M. Liang, M. Kohli, S. N. Thibodeau, L. Boardman, L. Wang, Characterization of human plasma-derived exosomal RNAs by deep sequencing. *BMC Genomics* **14**, 319 (2013).
19. E. N. M. Nolte-'t Hoen, H. P. J. Buermans, M. Waasdorp, W. Stoorvogel, M. H. M. Wauben, P. A. C. 't Hoen, Deep sequencing of RNA from immune cell-derived vesicles uncovers the selective incorporation of small non-coding RNA biotypes with potential regulatory functions. *Nucleic Acids Res.* **40**, 9272–9285 (2012).
20. C. P. Christov, T. J. Gardiner, D. Szüts, T. Krude, Functional requirement of noncoding Y RNAs for human chromosomal DNA replication. *Mol. Cell. Biol.* **26**, 6993–7004 (2006).
21. S. Sim, D. E. Weinberg, G. Fuchs, K. Choi, J. Chung, S. L. Wolin, The subcellular distribution of an RNA quality control protein, the Ro autoantigen, is regulated by noncoding Y RNA binding. *Mol. Biol. Cell* **20**, 1555–1564 (2009).

22. M. P. Kowalski, T. Krude, Functional roles of non-coding Y RNAs. *Int. J. Biochem. Cell Biol.* **66**, 20–29 (2015).
23. F. E. Nicolas, A. E. Hall, T. Csorba, C. Turnbull, T. Dalmay, Biogenesis of Y RNA-derived small RNAs is independent of the microRNA pathway. *FEBS Lett.* **586**, 1226–1230 (2012).
24. Y.-Y. Yeh, H. G. Ozer, A. M. Lehman, K. Maddocks, L. Yu, A. J. Johnson, J. C. Byrd, Characterization of CLL exosomes reveals a distinct microRNA signature and enhanced secretion by activation of BCR signaling. *Blood* **125**, 3297–3305 (2015).
25. A. K. Ghosh, C. R. Secreto, T. R. Knox, W. Ding, D. Mukhopadhyay, N. E. Kay, Circulating microvesicles in B-cell chronic lymphocytic leukemia can stimulate marrow stromal cells: Implications for disease progression. *Blood* **115**, 1755–1764 (2010).
26. J. Paggetti, F. Haderk, M. Seiffert, B. Janji, U. Distler, W. Ammerlaan, Y. J. Kim, J. Adam, P. Lichter, E. Solary, G. Berchem, E. Moussay, Exosomes released by chronic lymphocytic leukemia cells induce the transition of stromal cells into cancer-associated fibroblasts. *Blood* **126**, 1106–1117 (2015).
27. F. Haderk, B. Hanna, K. Richter, M. Schnölzer, T. Zenz, S. Stilgenbauer, P. Lichter, M. Seiffert, Extracellular vesicles in chronic lymphocytic leukemia. *Leuk. Lymphoma* **54**, 1826–1830 (2013).
28. T. Aung, B. Chapuy, D. Vogel, D. Wenzel, M. Oppermann, M. Lahmann, T. Weinhage, K. Menck, T. Hupfeld, R. Koch, L. Trümper, G. G. Wulf, Exosomal evasion of humoral immunotherapy in aggressive B-cell lymphoma modulated by ATP-binding cassette transporter A3. *Proc. Natl. Acad. Sci. U.S.A.* **108**, 15336–15341 (2011).
29. V. Balatti, Y. Pekarky, C. M. Croce, Role of microRNA in chronic lymphocytic leukemia onset and progression. *J. Hematol. Oncol.* **8**, 12 (2015).
30. G. A. Calin, M. Ferracin, A. Cimmino, G. Di Leva, M. Shimizu, S. E. Wojcik, M. V. Iorio, R. Visone, N. I. Sever, M. Fabbri, R. Iuliano, T. Palumbo, F. Pichiorri, C. Roldo, R. Garzon, C. Sevignani, L. Rassenti, H. Alder, S. Volinia, C.-g. Liu, T. J. Kipps, M. Negrini, C. M. Croce, A microRNA signature associated with prognosis and progression in chronic lymphocytic leukemia. *N. Engl. J. Med.* **353**, 1793–1801 (2005).
31. J. M. Dhahbi, S. R. Spindler, H. Atamna, D. Boffelli, P. Mote, D. I. K. Martin, 5′-YRNA fragments derived by processing of transcripts from specific YRNA genes and pseudogenes are abundant in human serum and plasma. *Physiol. Genomics* **45**, 990–998 (2013).
32. J. P. Tosar, F. Gámbaro, J. Sanguinetti, B. Bonilla, K. W. Witwer, A. Cayota, Assessment of small RNA sorting into different extracellular fractions revealed by high-throughput sequencing of breast cell lines. *Nucleic Acids Res.* **43**, 5601–5616 (2015).
33. M. Köhn, N. Pazaitis, S. Hüttelmaier, Why YRNAs? About versatile RNAs and their functions. *Biomolecules* **3**, 143–156 (2013).
34. C. P. Christov, E. Trivier, T. Krude, Noncoding human Y RNAs are overexpressed in tumours and required for cell proliferation. *Br. J. Cancer* **98**, 981–988 (2008).
35. M. Fabbri, A. Paone, F. Calore, R. Galli, E. Gaudio, R. Santhanam, F. Lovat, P. Fadda, C. Mao, G. J. Nuovo, N. Zanesi, M. Crawford, G. H. Ozer, D. Wernicke, H. Alder, M. A. Caligiuri, P. Nana-Sinkam, D. Perrotti, C. M. Croce, microRNAs bind to Toll-like receptors to induce prometastatic inflammatory response. *Proc. Natl. Acad. Sci. U.S.A.* **109**, E2110–E2116 (2012).
36. U. Klein, M. Lia, M. Crespo, R. Siegel, Q. Shen, T. Mo, A. Ambesi-Impiombato, A. Califano, A. Migliazza, G. Bhagat, R. Dalla-Favera, The *DLEU2/miR-15a/16-1* cluster controls B cell proliferation and its deletion leads to chronic lymphocytic leukemia. *Cancer Cell* **17**, 28–40 (2010).
37. F. Heil, H. Hemmi, H. Hochrein, F. Ampenberger, C. Kirschning, S. Akira, G. Lipford, H. Wagner, S. Bauer, Species-specific recognition of single-stranded RNA via Toll-like receptor 7 and 8. *Science* **303**, 1526–1529 (2004).
38. S. T. Sarvestani, B. R. G. Williams, M. P. Gantier, Human Toll-like receptor 8 can be cool too: Implications for foreign RNA sensing. *J. Interferon Cytokine Res.* **32**, 350–361 (2012).
39. M. C. Boelens, T. J. Wu, B. Y. Nabet, B. Xu, Y. Qiu, T. Yoon, D. J. Azzam, C. T.-S. Victor, B. Z. Wiemann, H. Ishwaran, P. J. ter Brugge, J. Jonkers, J. Slingerland, A. J. Minn, Exosome transfer from stromal to breast cancer cells regulates therapy resistance pathways. *Cell* **159**, 499–513 (2014).
40. A. Kužnik, M. Benčina, U. Švajger, M. Jeras, B. Rozman, R. Jerala, Mechanism of endosomal TLR inhibition by antimalarial drugs and imidazoquinolines. *J. Immunol.* **186**, 4794–4804 (2011).
41. D. Koppers-Lalic, M. Hackenberg, I. V. Bijnsdorp, M. A. J. van Eijndhoven, P. Sadek, D. Sie, N. Zini, J. M. Middeldorp, B. Ylstra, R. X. de Menezes, T. Würdinger, G. A. Meijer, D. M. Pegtel, Nontemplated nucleotide additions distinguish the small RNA composition in cells from exosomes. *Cell Rep.* **8**, 1649–1658 (2014).
42. B. W. M. van Balkom, A. S. Eisele, D. M. Pegtel, S. Bervoets, M. C. Verhaar, Quantitative and qualitative analysis of small RNAs in human endothelial cells and exosomes provides insights into localized RNA processing, degradation and sorting. *J. Extracell. Vesicles* **4**, 26760 (2015).
43. L. Vojtech, S. Woo, S. Hughes, C. Levy, L. Ballweber, R. P. Sauteraud, J. Strobl, K. Westerberg, R. Gottardo, M. Tewari, F. Hladik, Exosomes in human semen carry a distinctive repertoire of small non-coding RNAs with potential regulatory functions. *Nucleic Acids Res.* **42**, 7290–7304 (2014).
44. A. Forsbach, J. G. Nemorin, C. Montino, C. Müller, U. Samulowitz, A. P. Vicari, M. Jurk, G. K. Mutwiri, A. M. Krieg, G. B. Lipford, J. Vollmer, Identification of RNA sequence motifs stimulating sequence-specific TLR8-dependent immune responses. *J. Immunol.* **180**, 3729–3738 (2008).
45. A. G. Arimbasseri, K. Rijal, R. J. Maraia, Transcription termination by the eukaryotic RNA polymerase III. *Biochim. Biophys. Acta* **1829**, 318–330 (2013).
46. M. Tkach, C. Théry, Communication by extracellular vesicles: Where we are and where we need to go. *Cell* **164**, 1226–1232 (2016).
47. P. D. Robbins, A. Dorronsoro, C. N. Booker, Regulation of chronic inflammatory and immune processes by extracellular vesicles. *J. Clin. Investig.* **126**, 1173–1180 (2016).
48. L. Lagneaux, A. Delforge, M. Dejeneffe, M. Massy, M. Bernier, D. Bron, Hydroxychloroquine-induced apoptosis of chronic lymphocytic leukemia involves activation of caspase-3 and modulation of Bcl-2/bax/ratio. *Leuk. Lymphoma* **43**, 1087–1095 (2002).
49. S.-S. Chen, M. Kaufman, A. Caramanica, R. N. Damle, P. Garofalo, P. Ly, D. Janson, S. L. Allen, J. Kolitz, L. Quill, K. R. Rai, N. Chiorazzi, Efficacy and safety of hydroxychloroquine sulphate in chronic lymphocytic leukemia: Clinical trial experience in untreated patients. *Blood* **116**, 1392–1392 (2010).
50. C. J. Blume, A. Hotz-Wagenblatt, J. Hüllein, L. Sellner, A. Jethwa, T. Stolz, M. Slabicki, K. Lee, A. Sharathchandra, A. Benner, S. Dietrich, C. C. Oakes, P. Dreger, D. te Raa, A. P. Kater, A. Jauch, O. Merkel, M. Oren, T. Hielscher, T. Zenz, p53-dependent non-coding RNA networks in chronic lymphocytic leukemia. *Leukemia* **29**, 2015–2023 (2015).
51. Y. Liao, G. K. Smyth, W. Shi, featureCounts: An efficient general purpose program for assigning sequence reads to genomic features. *Bioinformatics* **30**, 923–930 (2014).
52. M. I. Love, W. Huber, S. Anders, Moderated estimation of fold change and dispersion for RNA-seq data with DESeq2. *Genome Biol.* **15**, 550 (2014).
53. H. Hemmi, T. Kaisho, O. Takeuchi, S. Sato, H. Sanjo, K. Hoshino, T. Horiuchi, H. Tomizawa, K. Takeda, S. Akira, Small anti-viral compounds activate immune cells via the TLR7 MyD88–dependent signaling pathway. *Nat. Immunol.* **3**, 196–200 (2002).
54. Q. Sun, L. Sun, H.-H. Liu, X. Chen, R. B. Seth, J. Forman, Z. J. Chen, The specific and essential role of MAVS in antiviral innate immune responses. *Immunity* **24**, 633–642 (2006).

Acknowledgments: We thank M. Schnölzer, K. Richter, V. Thewes, N. Diessl, A. Stephan, and S. Ohl [all from the German Cancer Research Center (DKFZ), Heidelberg] for advice and contributions, as well as S. Bauer (Philipps University of Marburg, Germany) for provision of mice. **Funding:** This study was supported by the Cooperation Program in Cancer Research of the DKFZ and Israel's Ministry of Science, Technology and Space, by the German José Carreras Foundation (R12/27), by the Helmholtz Virtual Institute ("Understanding and overcoming resistance to apoptosis and therapy in leukemia"), by the Federal Ministry for Education and Research (BMBF) Networks "CancerEpiSys" (0316049C) and "PRECiSe" (031L0076A), by the Else Kröner–Fresenius Foundation, by Télévie (7.4563.15), and by the Luxembourg Institute of Health (HEMATEXO). **Author contributions:** F.H. and M.S. designed the study, analyzed the data, and wrote the manuscript. F.H., R.S., L.L.C., T.W., K.V.W., and A.S. conducted the experiments. M.I. and M.Z. performed bioinformatic analyses. M.N. conducted electron microscopy analyses. U.W. performed analyses of proteome data. A.B. performed statistical analyses and provided heat maps. M.G., J.D., T.Z., and S.S. provided clinical samples. J.S., S.D., J.P., E.M., M.Z., and P.L. were involved in discussions regarding experimental protocols and data. M.S. and P.L. provided logistic and budget support. **Competing interests:** The authors declare that they have no competing interests. **Data and materials availability:** The mass spectrometry proteomics data of CLL and healthy donor plasma exosomes have been deposited to the ProteomeXchange Consortium via the PRIDE partner repository with the data set identifier PXD004420 (www.ebi.ac.uk/pride). The RNA sequencing data from MEC-1 cells and exosomes have been deposited in the National Center for Biotechnology Information's Gene Expression Omnibus (GEO) and are accessible through GEO Series accession number GSE83539 (www.ncbi.nlm.nih.gov/geo/query/acc.cgi?token=wbkrcumqthkxfct&acc=GSE83539). The raw RNA sequencing data of plasma exosomes from three CLL patients are available from the European Genome-phenome Archive with the accession ID EGAD00001003230 (www.ebi.ac.uk/ega/datasets/EGAD00001003230).

Submitted 13 July 2016
Resubmitted 23 March 2017
Accepted 12 June 2017
Published 28 July 2017
10.1126/sciimmunol.aah5509

Citation: F. Haderk, R. Schulz, M. Iskar, L. L. Cid, T. Worst, K. V. Willmund, A. Schulz, U. Warnken, J. Seiler, A. Benner, M. Nessling, T. Zenz, M. Göbel, J. Dürig, S. Diederichs, J. Paggetti, E. Moussay, S. Stilgenbauer, M. Zapatka, P. Lichter, M. Seiffert, Tumor-derived exosomes modulate PD-L1 expression in monocytes. *Sci. Immunol.* **2**, eaah5509 (2017).

Science Immunology

Tumor-derived exosomes modulate PD-L1 expression in monocytes

Franziska Haderk, Ralph Schulz, Murat Iskar, Laura Llaó Cid, Thomas Worst, Karolin V. Willmund, Angela Schulz, Uwe Warnken, Jana Seiler, Axel Benner, Michelle Nessling, Thorsten Zenz, Maria Göbel, Jan Dürig, Sven Diederichs, Jérôme Paggetti, Etienne Moussay, Stephan Stilgenbauer, Marc Zapatka, Peter Lichter and Martina Seiffert

Sci. Immunol. **2**, eaah5509.
DOI: 10.1126/sciimmunol.aah5509

Messaging with RNAs

Understanding interactions between tumor cells and immune cells is essential for tailoring immunocentric therapies to tumors. Here, Haderk *et al*. have identified a key role for tumor-derived exosomes in modulating immune responses to chronic lymphocytic leukemia (CLL). They report that CLL-derived exosomal RNAs promote monocytes in CLL patients to adopt an immunosuppressive phenotype, including promoting expression of PD-L1. They identify noncoding RNA hY4 as a key functional component of CLL-derived exosomes and show that hY4 promotes exosome-dependent skewing of monocytes in a TLR7-dependent manner. Using mouse models, they found that inhibition of TLR7 delayed progression of CLL, opening up the possibility that the TLR7 pathway could be therapeutically targeted in CLL.